

Characterization of the cytotoxic properties of the benzimidazole fungicides, benomyl and carbendazim, in human tumour cell lines and primary cultures of patient tumour cells

Daniel Laryea^a, Joachim Gullbo^a, Anders Isaksson^a, Rolf Larsson^a and Peter Nygren^b

The benzimidazoles, benomyl and carbendazim, are fungicides suggested to target microtubules. Benomyl is metabolized to carbendazim, which has already been explored as an anticancer drug in phase 1 clinical trials. We further characterized the cytotoxic properties of benomyl and carbendazim in 12 human cell lines and in primary cultures of patient tumour cells with the overall aims of elucidating mechanisms of action and anticancer activity spectrum. Cytotoxicity was assessed in the short-term fluorometric microculture cytotoxicity assay and was correlated with the activity of other anticancer drugs and gene expression assessed by cDNA microarray analysis. Benomyl was generally more potent than its metabolite, carbendazim. Both showed high drug activity correlations with several established and experimental anticancer drugs, but modest association with established mechanisms of drug resistance. Furthermore, these benzimidazoles showed high correlations with genes considered relevant for the activity of several mechanistically different standard and experimental anticancer drugs, indicating multiple and broad

mechanisms of action. In patient tumour samples, benomyl tended to be more active in haematological compared with solid tumour malignancies, whereas the opposite was observed for carbendazim. In conclusion, benomyl and carbendazim show interesting and diverse cytotoxic mechanisms of action and seem suitable as lead compounds for the development of new anticancer drugs. *Anti-Cancer Drugs* 21:33–42 © 2010 Wolters Kluwer Health | Lippincott Williams & Wilkins.

Anti-Cancer Drugs 2010, 21:33–42

Keywords: benomyl, carbendazim, cross-resistance, cytotoxic drug, gene expression, tumour cell

Departments of ^aMedical Sciences, Division of Clinical Pharmacology and ^bOncology, Radiology and Clinical Immunology, Division of Oncology, Uppsala University Hospital, Uppsala, Sweden

Correspondence to Dr Daniel Laryea, Department of Medical Sciences, Division of Clinical Pharmacology, Uppsala University Hospital, Entrance 61 4th Floor, Uppsala S-751 85, Sweden
Tel: +46 18 6115959; fax: +46 18 6113703;
e-mail: daniel.laryea@medsci.uu.se

Received 13 May 2009 Revised form accepted 16 July 2009

Introduction

Benzimidazoles are a chemical group used as lead compounds for drugs against fungi, helminthes and peptic ulcers. Benomyl and carbendazim belong to this chemical group and are widely used as fungicides [1]. However, the suggested mechanism of action of these agents, disruption of microtubule turn-over, has made benomyl and carbendazim attractive for development into anticancer drugs. Clinical phase 1 studies on orally administered carbendazim [2,3] showed some anticancer activity at insignificant toxicity. Carbendazim was concluded to be a promising new agent in need of a new formulation to allow for further dose escalation. These findings provide the rationale for further investigations into the anticancer properties of benomyl and carbendazim as undertaken here.

Benomyl differs structurally from its major metabolite carbendazim by the butylcarbamoil side chain, whereas they have the benzimidazole ring in common (Fig. 1). The side chain is known to produce the active metabolite,

n-butyl isocyanate, which is conjugated to intermediaries bioactivated to form thiocarbamates that might also contribute to the normal tissue effects of benomyl as shown *in vivo* [4] and probably elicit anticancer activity as well.

Using gene expression profiling on the basis of microarrays to further characterize possible mechanisms of activity, this study seeks to expand the data on benomyl and carbendazim to expand the basis for their development as novel anticancer agents.

Materials and methods

Cell lines and cell culture

The cell line panel used consists of 12 different human cell lines. Key characteristics of the cell line panel are provided in Table 1.

The cells were grown in a culture medium, RPMI-1640 (Sigma Chemical Co., St Louis, Missouri, USA), supplemented with 10% heat-inactivated foetal calf serum, 2 mmol/l glutamine, 50 µg/ml streptomycin and 60 µg/ml

penicillin (all from Sigma). The CEM/VM-1 cell line was cultured in drug-free medium and was grown for 3–4 months without loss of resistance. U-937/Vcr was cultured continuously in the presence of 10 ng/ml vincristine. 8226/Dox40 was exposed once monthly to 0.24 µg/ml of doxorubicin and 8226/LR5 was exposed to 1.53 µg/ml melphalan when changing medium. NCI-H69AR was fed alternately with drug-free medium and a medium that contained 0.46 µg/ml doxorubicin. The drug-resistant sublines were routinely tested to ascertain the maintenance of their resistance phenotypes. hTERT-RPE1 was cultured in Dulbecco's modified Eagle's medium nutrient F-12 Ham, and HeLa in Eagle minimal essential medium, both with supplements as described above. The HeLa medium was also supplemented with 1 mmol/l sodium pyruvate. All cell lines were kept in a humidified incubator with 5% carbon dioxide at 37°C. Cell growth and morphology were monitored weekly. Cells were split twice a week and were harvested for the experiments when at log phase.

Patient tumour cells

Tumour samples from patients for the investigation of the activity of benomyl and carbendazim were obtained at diagnostic biopsy, routine surgery or bone marrow biopsy/peripheral blood sampling. The tumour sampling was approved by the Local Ethics Committee at Uppsala University. It was not possible to retrieve details on earlier treatment status for the patient samples included. However, most haematological samples were from untreated patients and most solid tumour samples were from previously treated patients. There were 30 samples

of haematological malignancies, including acute lymphoblastic leukaemia ($n = 8$), acute myelocytic leukaemia ($n = 6$), chronic lymphocytic leukaemia ($n = 7$) and non-Hodgkin's lymphoma ($n = 9$). There were 34 samples from solid tumours, including cancer of the ovary ($n = 14$), breast ($n = 5$), colon or rectum ($n = 5$), kidney ($n = 6$) and four samples from non-small-cell lung cancer. In addition, peripheral blood mononuclear cells isolated from five healthy blood donors were used as reference normal cells.

Haematological tumour cells were isolated from bone marrow or peripheral blood by using density gradient centrifugation [5] with 1.007 g/ml Ficoll-Paque (Pharmacia Biotech, Uppsala, Sweden). In preparing cells from solid tumour, tissue from the latter was minced into millimetre-sized pieces and were then digested in collagenase, and purified by using Percoll (Pharmacia Biotech) and density gradient centrifugation as described earlier [5]. All preparations had a cell viability greater than 90%, as judged by Trypan blue exclusion, and the proportion of tumour cells was greater than 70% according to May-Grünwald-Giemsa stained cytospin preparations assessed by a cytopathologist.

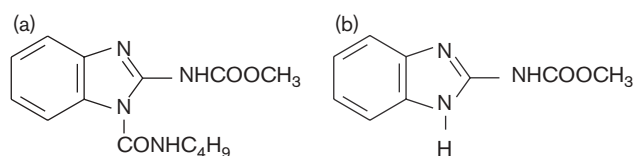
Exposure to cytotoxic drugs

In addition to benomyl and carbendazim, the cell lines were also tested against rapamycin, an mTOR inhibitor (Sigma Aldrich-Chemie, Steinheim, Germany) and the proteasome inhibitors disulfiram, lactacystin (Sigma Aldrich, St. Louis, Missouri, USA) and bortezomib (Velcade; Millennium Pharmaceuticals, Cambridge, Massachusetts, USA). In addition, the cell lines were tested earlier against a number of mechanistically different established and experimental cytotoxic agents using the same experimental setup [6,7]. These data were used for the assessment of cross-resistance and mechanistic considerations.

Culture plate preparation and measurement of drug activity

Dose-response 384-well plates (Nunc, Roskilde, Denmark) for the measurement of cytotoxicity were prepared assisted by a pipetting robot (Biomek 2000; Beckman Coulter Inc., Fullerton, California, USA). All drugs were dissolved according to the manufacturers' instructions to stock solutions at 10-times the final highest experimental

Fig. 1



Chemical structures of (a) benomyl (methyl 1-(butylcarbamoyl)-2-benzimidazole carbamate) and (b) carbendazim (methyl-2-benzimidazole carbamate).

Table 1 Characteristics of the human tumour cell line panel

Parental cell line	Histological origin	Resistant subline	Drug used for resistance selection	Resistance mechanism (MDR)
CCRF-CEM	T-cell leukaemia	CEM/VM-1	Teniposide	Topoisomerase-II-associated
RPMI 8226-S	Multiple myeloma	8226/Dox	Doxorubicin	P-gp170-associated
RPMI 8226-S	Multiple myeloma	8226/LR5	Melphalan	GSH-associated
U-937-GTB	Histiocytic lymphoma	U-937/Vcr	Vincristine	Tubulin-associated
NCI-H69	Small cell lung cancer	H69/AR	Doxorubicin	MRP1
ACHN	Renal adenocarcinoma	None	NA	NA
hTERT-RPE1	Normal retinal epithelia cells	None	NA	NA
HeLa	Cervical adenocarcinoma	None	NA	NA

For further details on the characteristics of the human tumour cell line panel, see Ref. [8].

GSH, reduced glutathione; MDR, multidrug resistance; NA, not applicable; MRP1, multidrug resistance-related protein 1 (also termed ABCC1); P-gp, P-glycoprotein.

concentration, and were then 10-fold serially diluted in five steps and suspended at 5 µl/well using a pipetting robot (Bio-Tek Instruments, Winooski, Vermont, USA). The plates were kept at -80°C and thawed immediately before the experiments. Cell suspension of 45 µl with 2500 (cell lines) or 5000 (patient samples) cells was seeded into each well of the drug-prepared plates using an automated Precision 2000 robot (Bio-Tek Instruments). Two columns with cells without drugs served as controls and two columns containing culture medium only served as blanks. The plates were incubated in 5% CO_2 at 37°C for 72 h before the assessment of cytotoxicity in the fluorometric microculture cytotoxicity assay.

Briefly, after culture the plates were washed followed by addition of 50 µl per well of 0.5 mg/ml fluorescein diacetate (FDA; Sigma) in PBS. After 40 min of incubation, the fluorescence was measured in a fluorometer (FLUORstar optima; BMG Labtechnologies, Offenburg, Germany). The nonfluorescent fluorescein diacetate, FDA, was hydrolysed to fluorescent fluorescein by viable cells with intact plasma membrane, and the fluorescence was quantified in a fluorometer. Thus, fluorescence after drug treatment is correlated to the number of viable cells [6].

Gene expression analysis

The cell line panel was characterized earlier in our laboratory for gene expression by microarray analysis [7], and these data were used in this study for the analysis of the relationship between drug activity and gene expression. Briefly, total RNA was extracted from each cell line starting from 10^7 cells, and only pure RNA without any signs of degradation was used in the subsequent experiments. The microarrays were printed in house and included 7458 cDNA clones as detailed at http://www.medsci.uu.se/klinfarm/arrayplatform/cDNA_array.htm.

Each cell line was analysed on two separate arrays with genes printed in duplicates on each array and with the Cy3 and Cy5 dyes reversed, providing a total of four measurements per gene and cell line. Genes with missing values for more than half of the cell lines were removed from the data set, reducing the number of genes from 7458 to 3903. The microarrays were scanned using a GenePix 4000B scanner (Axon Instruments, Union City, California, USA). The images were analysed and raw data were normalized. The average expression level for each gene and sample was then calculated and transformed to \log_2 values. The \log_2 value of the gene expression for each cell line was incorporated into the drug database and a correlation analysis was performed.

Pearson's correlation coefficients for all drug–drug ($\log_{10}\text{IC}_{50}$), gene–gene (\log_2) and drug–gene correlations were calculated. The complete list of the CloneIDs was fed into the SOURCE interface (check link above) after which gene information was retrieved for analyses.

Of the 3903 genes reported for all cell lines, 306 and 186 genes were found associated with the activity of benomyl, and 269 and 263 genes with the activity of carbendazim based on cut-off correlation coefficients of ≥ 0.70 and ≤ -0.70 , respectively. Complete lists of these genes are available at <http://www.medsci.uu.se/klinfarm/BenoCarb.htm>.

Data analysis and presentation

Fluorometric microculture cytotoxicity assay data are presented as percentage of survival index (SI), defined as the fluorescence of experimental wells in percentage of control wells with blank values subtracted. Dose–response data for cell lines are presented as means \pm SEM of three independent experiments, with duplicate wells for each drug concentration. The IC_{50} value for each drug in each cell line was obtained from concentration–response curves constructed in Excel (Microsoft, Informer Technologies Inc., USA) and GraphPad Prism (GraphPad Software Inc., California, USA). Quality criteria for a successful assay were judged from control wells where the fluorescence signal should be more than 10 times the mean blank value and the mean coefficient of variation less than 30%.

Delta graph for an individual cell line and drug were obtained by subtracting its $\log_{10}\text{IC}_{50}$ from the mean $\log_{10}\text{IC}_{50}$ of all the cell lines included. These deltas are presented graphically with bars deviating to the left from zero for tumour cell lines that are relatively more sensitive, and those deviating to the right relatively more resistant than the average. These delta bar graphs provide ‘fingerprints’ for the activity pattern of an individual drug.

Table 2 provides information on selected genes with expression correlation coefficients ≥ 0.70 or ≥ -0.70 to the activity of benomyl or carbendazim. Selection of these genes, some of which were discussed, was based on proposed molecular cytotoxic mechanisms of benomyl or carbendazim, current knowledge on genes frequently involved in anticancer drug activity, genes involved in drug sensitivity and resistance in breast cancer, in which carbendazim was relatively most active among solid tumour types, and genes considered to be involved in the activity of drugs to which benomyl or carbendazim showed high correlation in this study.

Table 3 shows a list of drug activity–gene expression correlations for groups of genes described to be related to the indicated cytotoxic drug mechanistic groups. This allows for comparison of the mechanistic profile between the drugs with gene correlations expected to be high for drugs considered to have that mechanism of action. The mean absolute values of the individual correlation coefficients were calculated to simplify the comparison between drugs.

Statistical inferences were calculated using the two-tailed Wilcoxon's matched-pairs test or, for unpaired data, the

Table 2 Selected genes with correlation coefficient for benomyl or carbendazim of ≥ 0.7 or ≤ -0.7

ACC ID	Gene	Correlation coefficients		Rank
		Benomyl	Carbendazim	
884438	Nuclear factor (erythroid-derived 2)-like 2 (<i>Nrf2</i>)	0.8775	0.9375	1
814899	BCL-2/adenovirus E1B	0.8109	0.8899	2
786680	Annexin A5	0.9387	0.8829	3
745604	Breast cancer anti-estrogen resistance 1 (<i>BRCA1</i>)	0.9356	0.8735	4
429574	Caspase 3, apoptosis-related cysteine peptidase	0.8213	0.8718	5
2113597	Phosphoinositide-3-kinase, class 2, alpha	0.7705	0.8707	6
435948	Aldo-keto reductase family 1	0.8634	0.8695	7
796694	Effector cell peptidase receptor 1 (Survivin) (<i>BIRC5</i>)	0.7143	0.8682	8
435953	Inositol 1,4,5-triphosphate receptor, type 3	0.7278	0.863	9
897567	Lactate dehydrogenase A	0.6178	0.8624	10
461525	F-box and WD-40 repeat domain containing 11	0.5969	0.8623	11
506646	TP53 activated protein 1 (<i>TP53AP1</i>)	0.6954	0.861	12
1573778	Ras association domain family 7	0.7887	0.8546	13
592125	Receptor (TNFRSF)-interacting serine-threonine kinase 1	0.6206	0.8236	14
795198	Solute carrier family 39 (zinc transporter), member 1	0.8121	0.8093	15
897806	Hypoxia-inducible factor 1, alpha subunit (<i>HIF 1A</i>)	0.7738	0.7951	16
2149720	Kinesin family member 1C	0.8385	0.7938	17
814961	Ubiquitin specific peptidase 5 (isopeptidase T)	0.6803	0.7898	18
2066352	V-erb-b2 erythroblastic leukaemia viral oncogene.	0.8052	0.7769	19
292212	ATP-binding cassette, subfamily C member 5 (<i>ABCC5</i>)	0.813	0.7727	20
325062	Solute carrier family 20 member 1	0.8415	0.7622	21
1071197	Cyclin D1	0.8169	0.7606	22
2430680	Mitogen-activated protein kinase 11	0.7407	0.7569	23
1057969	Retinoblastoma 1 (including osteosarcoma)	0.7961	0.7507	24
855624	Aldehyde dehydrogenase 1 family, member A1	0.7888	0.739	25
324861	Epidermal growth factor receptor oncogene (<i>EGFR</i>)	0.8746	0.7248	26
279670	Breast cancer anti-estrogen resistance 3 (<i>BRCA3</i>)	0.8545	0.7075	27
271416	Sp1 Transcription factor	0.5393	0.7022	28
855707	Overexpressed in colon carcinoma 1 (<i>OCC-1</i>)	0.721	0.6333	29
324225	Retinoic acid receptor responder 3	0.7989	0.5791	30
684661	GLI pathogenesis-related 1 (glioma)	0.7000	0.3919	31
740780	Kallikrein-related peptidase 11	-0.8787	-0.9353	1
254029	Serine/threonine protein kinase	-0.6935	-0.9306	2
2019211	RAS-associated protein (<i>RAB 33A</i>)	-0.9108	-0.923	3
770588	Zinc finger protein	-0.7027	-0.9078	4
727192	Nuclear factor of activated T-cells (<i>NFAT</i>)	-0.7517	-0.9069	5
1133751	MYC binding protein 2	-0.8014	-0.9035	6
257445	Ubiquitin carboxyl terminal esterase L3	-0.6958	-0.8987	7
47900	Interferon gamma receptor 1	-0.6912	-0.8964	8
1558151	Basic leucine zipper transcription factor, ATF-like	-0.6854	-0.8937	9
704905	RAS-related protein 1A (<i>RAP 1A</i>)	-0.6745	-0.8833	10
1519230	Serologically defined colon cancer antigen 10 <i>SDCCAG10</i>	-0.9048	-0.8753	11
593690	Tumour necrosis factor (ligand) superfamily 13B	-0.6281	-0.8716	12
2505796	Cytochrome C oxidase subunit Vb	-0.8033	-0.8635	13
780947	Polymerase (DNA-directed) delta 1	-0.9067	-0.8562	14
1915749	Glia maturation factor, gamma	-0.8122	-0.8471	15
841617	Ornithine decarboxylase antizyme 1	-0.6575	-0.846	16
49303	Protein phosphatase 2, regulatory subunit B, beta isoform	-0.5608	-0.817	17
343871	Mitogen-activated protein kinase kinase 5	-0.7998	-0.8085	18
2306860	MAD 2 mitotic arrest	-0.894	-0.8077	19
342647	Mitogen-activated protein kinase-activated	-0.6293	-0.8068	20
768043	Evolutionary-conserved signalling intermediate in TOLL pathway	-0.7777	-0.7982	21
461522	ATP-binding cassette, subfamily B, member 7 (<i>ABCB7</i>)	-0.8503	-0.7844	22
700527	Glutaredoxin (<i>GLRX</i>)	-0.4496	-0.7758	23
235938	BCL-2-antagonist/killer 1 (<i>BAK1</i>)	-0.6687	-0.7493	24
869442	Thioredoxin 2 (<i>TXN2</i>)	-0.4572	-0.741	25
49410	Catalase (<i>CAT</i>)	-0.3477	-0.7221	26
757404	Von Hippel-Lindau binding protein 1	-0.829	-0.722	27
341763	Caspase 5, apoptosis-related cysteine peptidase	-0.4089	-0.7061	28
502369	Programmed cell death 5 <i>PDCD5</i>	-0.8154	-0.6629	29
1468820	Nitric oxide synthase <i>NOS3</i>	-0.7393	-0.6065	30
950592	FK506 binding protein 12-rapamycin associated protein 1	-0.7006	-0.493	31

Ranking of the genes was based on the correlations for carbendazim.

ACC ID, accession identity.

Mann-Whitney test. Statistical analysis was performed using GraphPad Prism (GraphPad Software). Resistance factor (RF) was calculated by dividing the IC_{50} for a drug in a resistant subline with the IC_{50} of its parental cell line [8].

Results

Cell lines

Drug potency and activity correlations

Benomyl was more potent than carbendazim in the cell lines, but the pattern of differential activity in the cell

Table 3 Drug activity–gene expression correlations for genes selected for their association with some well-known cytotoxic drug mechanistic groups and for the individual drugs indicated

ACCID	Tubulin	Test		Tubulin			Topoisomerase			Anti-metabolite		Alkylating		Proteas	Methylating	Ox stress
	Gene	Beno	Carb	Colch	Vinc	Paclit	Dox	Etopo	Mitoxan	5-FU	Gem	Cis	Melph	Bortez	Decitab	Rotenone
745138	<i>TUBA3D</i>	0.54	0.56	0.72	0.69	0.29	0.52	0.50	0.36	0.67	0.60	0.34	0.16	0.27	0.25	0.79
810741	<i>GABARAP</i>	0.59	0.37	0.71	0.85	0.47	0.58	0.42	0.01	0.76	0.58	0.47	0.29	0.34	−0.18	0.68
1470060	<i>TUBA1A</i>	0.45	0.27	0.65	0.68	0.29	0.41	0.32	0.10	0.54	0.55	0.29	0.09	−0.11	−0.06	0.79
285736	<i>LATS2</i>	0.65	0.52	0.65	0.39	0.88	0.47	0.46	0.31	0.64	0.24	0.11	0.17	0.26	0.30	0.73
1340447	<i>BRCA2</i>	−0.18	−0.08	−0.64	−0.56	−0.11	−0.25	−0.16	0.05	−0.40	−0.54	−0.04	−0.33	−0.15	0.18	−0.28
384013	<i>NUDC</i>	−0.68	−0.54	−0.60	−0.65	−0.15	−0.46	−0.58	−0.45	−0.52	−0.72	−0.38	−0.91	−0.38	−0.38	−0.30
49229	<i>GPHN</i>	−0.08	0.06	−0.56	−0.56	−0.23	−0.17	−0.07	0.20	−0.35	−0.50	0.03	−0.31	−0.06	0.30	−0.19
296180	<i>RP2</i>	−0.50	−0.27	−0.52	−0.3	−0.25	−0.23	−0.13	−0.20	−0.05	−0.29	−0.03	−0.75	−0.28	−0.14	−0.08
Mean absolute correlation		0.46	0.34	0.63	0.63	0.33	0.38	0.33	0.21	0.49	0.50	0.21	0.37	0.23	0.22	0.48
Topoisomerase																
814109	<i>POLS</i>	0.12	0.32	0.13	0.45	0.01	0.21	0.39	0.16	0.63	0.46	0.26	−0.09	0.45	0.18	0.25
773254	<i>SFPQ</i>	0.15	0.42	−0.07	−0.17	−0.28	−0.05	0.27	0.62	−0.03	0.12	0.09	0.09	0.05	0.73	0.15
2437558	<i>TOP3B</i>	−0.56	−0.33	−0.66	−0.13	−0.71	−0.30	−0.13	−0.17	−0.16	0.04	0.05	−0.27	−0.09	−0.14	−0.56
1371498	<i>MLL</i>	−0.19	−0.42	0.02	−0.21	−0.02	−0.41	−0.26	−0.31	0.04	0.08	−0.52	−0.10	−0.67	−0.33	0.02
79436	<i>TOP2B</i>	−0.78	−0.87	−0.62	−0.46	−0.55	−0.77	−0.72	−0.80	−0.40	−0.42	−0.44	−0.48	−0.54	−0.75	−0.64
825470	<i>TOP2A</i>	−0.36	−0.73	−0.26	−0.20	0.07	−0.39	−0.53	−0.82	−0.11	−0.36	−0.23	−0.40	−0.69	−0.83	−0.14
200136	<i>TOPBP1</i>	−0.51	0.08	−0.48	−0.52	0.04	0.01	−0.49	−0.48	−0.59	−0.57	−0.39	−0.35	−0.45	−0.52	−0.52
396320	<i>TOP3B</i>	−0.41	−0.26	−0.12	−0.21	0.25	−0.19	−0.28	−0.33	0.03	−0.26	−0.23	−0.80	−0.19	−0.28	0.15
Mean absolute correlation		0.39	0.43	0.29	0.29	0.24	0.29	0.39	0.46	0.25	0.29	0.28	0.32	0.39	0.47	0.30
DNA interaction																
811015	<i>FOS</i>	0.70	0.59	0.28	0.71	0.03	0.71	0.71	0.32	0.72	0.46	0.89	0.38	0.50	0.32	0.61
382564	<i>FOX D1</i>	0.77	0.67	0.25	0.70	0.06	0.70	0.74	0.43	0.62	0.50	0.87	0.55	0.43	0.76	0.59
161993	<i>CEBPB</i>	0.48	0.50	−0.21	0.25	0.03	0.44	0.49	0.23	0.39	−0.51	0.83	−0.35	0.44	0.31	0.38
810119	<i>SNAI1</i>	0.48	0.33	−0.05	0.59	−0.22	0.42	0.40	0.08	0.38	0.05	0.80	0.03	0.22	−0.10	−0.34
825478	<i>ZNF146</i>	−0.75	−0.74	−0.28	−0.49	0.03	−0.65	−0.80	−0.66	−0.50	−0.40	−0.78	−0.65	−0.40	−0.86	−0.49
31873	<i>HMG N4</i>	−0.48	−0.30	−0.20	−0.68	−0.27	−0.62	−0.61	0.02	−0.86	−0.20	−0.77	−0.20	−0.26	0.28	−0.59
789152	<i>ZNF75</i>	−0.66	−0.65	0.03	−0.28	−0.18	−0.41	−0.62	−0.53	−0.49	0.07	−0.75	−0.32	−0.55	−0.65	−0.34
810575	<i>ZNRD1</i>	−0.75	−0.69	−0.51	−0.57	−0.24	−0.57	−0.64	−0.38	−0.74	−0.19	−0.72	−0.04	−0.33	−0.38	−0.90
Mean absolute correlation		0.63	0.56	0.23	0.53	0.13	0.57	0.63	0.33	0.59	0.30	0.80	0.32	0.39	0.46	0.53
Methyltransferase																
842839	<i>METTL9</i>	0.70	0.82	0.50	0.18	0.52	0.43	0.43	0.67	0.22	0.06	0.24	0.22	0.52	0.75	0.64
280970	<i>NOL1</i>	0.05	0.35	0.15	−0.23	0.34	0.05	0.03	0.48	−0.18	0.15	−0.27	0.01	0.16	0.64	0.14
755302	<i>PRMT5</i>	0.13	0.22	0.16	−0.06	−0.08	−0.01	0.08	0.44	−0.14	0.33	−0.31	0.01	0.12	0.49	0.04
531319	<i>AURKB</i>	0.27	0.23	0.60	−0.19	0.68	−0.02	0.02	0.37	−0.01	0.07	−0.40	0.13	−0.25	0.49	0.60
782217	<i>NSUN4</i>	0.70	0.78	−0.35	−0.04	−0.09	−0.35	−0.55	−0.83	−0.14	−0.12	−0.29	−0.51	−0.35	0.86	−0.41
33616	<i>CABIN1</i>	0.78	0.87	−0.53	−0.64	−0.32	−0.75	−0.71	−0.80	−0.40	−0.63	−0.48	−0.67	−0.70	0.78	−0.46
841140	<i>ICMT</i>	0.26	0.35	−0.25	0.13	−0.01	−0.04	−0.24	−0.73	0.26	−0.42	0.24	−0.87	−0.11	0.77	0.19
594164	<i>SETD2</i>	0.35	0.65	−0.06	−0.29	0.16	−0.19	−0.51	−0.61	−0.34	−0.36	−0.34	−0.40	−0.78	0.74	−0.01
Mean absolute correlation		0.40	0.53	0.32	0.22	0.28	0.23	0.32	0.62	0.21	0.27	0.32	0.35	0.37	0.69	0.31
Histone deacetylase																
796114	<i>SIRT1</i>	0.50	0.58	0.44	0.33	0.49	0.40	0.58	0.73	0.29	0.58	−0.04	0.65	0.36	0.73	0.22
824074	<i>YY1</i>	0.19	0.39	0.25	−0.15	0.14	−0.14	−0.10	0.38	−0.15	0.13	−0.16	0.09	0.12	0.57	0.29
840766	<i>TBL1X</i>	0.02	0.04	0.27	−0.27	0.06	−0.37	−0.08	0.27	−0.16	0.37	−0.53	0.71	−0.06	0.55	−0.17
810552	<i>PHB2</i>	0.26	0.47	0.77	0.30	0.71	0.55	0.34	0.55	0.15	0.58	−0.19	0.32	0.34	0.46	0.42
502669	<i>HDAC2</i>	0.63	0.87	−0.48	−0.27	−0.11	−0.46	−0.66	−0.91	−0.25	−0.48	−0.37	−0.78	−0.71	0.94	−0.24
1556536	<i>SIRT7</i>	0.77	0.90	−0.38	−0.45	−0.00	−0.56	−0.81	−0.85	−0.50	−0.45	−0.60	−0.58	−0.59	0.93	−0.49

Table 3 (continued)

Tubulin		Test		Tubulin			Topoisomerase			Anti-metabolite		Alkylating		Proteas	Methylating	Ox stress
ACCID	Gene	Beno	Carb	Colch	Vinc	Pacit	Dox	Etopo	Mitoxan	5-FU	Gem	Cis	Melph	Bortez	Decitab	Rotenone
450912	SIRT2	0.57	0.73	-0.47	-0.01	-0.32	-0.34	-0.47	-0.87	0.03	-0.29	-0.02	-0.69	-0.44	0.91	-0.22
2549383	SIRT6	0.26	0.56	-0.04	0.04	0.13	-0.04	-0.19	-0.64	0.08	-0.19	-0.04	-0.50	-0.73	0.84	0.19
Mean absolute correlation		0.40	0.57	0.39	0.23	0.25	0.36	0.40	0.65	0.20	0.38	0.24	0.54	0.42	0.74	0.28
Oxidative stress																
859359	TP53/3	0.89	0.73	0.61	0.71	0.34	0.66	0.66	0.38	0.75	0.35	0.74	0.36	0.42	0.38	0.87
137940	GSTM3	0.54	0.67	0.57	0.50	0.36	0.49	0.54	0.54	0.68	0.38	0.61	0.12	0.73	0.57	0.84
781019	PON2	0.80	0.67	0.75	0.49	0.59	0.55	0.54	0.38	0.65	0.15	0.43	0.28	0.48	0.33	0.84
504527	DUSP1	0.91	0.72	0.60	0.69	0.43	0.69	0.67	0.39	0.73	0.26	0.71	0.43	0.52	0.36	0.81
2467229	PARK7	-0.39	-0.40	-0.32	-0.29	-0.30	-0.29	-0.48	-0.38	-0.55	-0.24	-0.18	0.13	0.07	-0.35	-0.72
502141	NDUFS8	-0.34	-0.17	0.01	0.04	-0.02	0.02	0.01	0.10	-0.17	0.62	-0.39	0.57	0.22	0.05	-0.66
82879	MBL2	-0.81	-0.83	-0.47	-0.60	-0.32	-0.88	-0.80	-0.74	-0.50	-0.38	-0.61	-0.39	-0.56	-0.71	-0.64
884455	PRDX5	-0.04	-0.12	-0.05	-0.12	-0.04	-0.10	-0.09	-0.10	-0.22	-0.03	-0.04	0.54	0.23	-0.06	-0.53
Mean absolute correlation		0.59	0.54	0.42	0.43	0.30	0.46	0.48	0.38	0.53	0.30	0.46	0.36	0.40	0.35	0.74

Drugs were categorized according to their established mechanisms of action. Mean values for the absolute correlation coefficients (bold) for each drug was calculated to simplify data interpretation. A few well-known cytotoxic drug mechanistic groups are also set in bold type. Beno, benomyl; Bortez, bortezomib; Carb, carbendazim; Cis, cisplatin; Decitab, decitabine; Dox, doxorubicin; Etopo, etoposide; 5-FU, 5-fluorouracil; Gemcit, gemcitabine; Melph, melphalan; Mitoxan, mitoxantrone; Ox stress, oxidative stress; Pacit, paclitaxel; Proteas, proteasome; Roten, rotenone; Vinc, vincristine

line panel was similar although carbendazim showed somewhat less difference in activity between haematological and solid tumour cell lines (Fig. 2). The mean IC₅₀ values in the cell lines were 15 ± 5.7 and 50 ± 9.0 µmol/l (mean ± SEM), for benomyl and carbendazim, respectively (*P* = 0, 0005).

Table 4 shows the correlations between benomyl or carbendazim and mechanistically different standard and experimental cytotoxic agents. High-to-moderate correlation coefficients were observed for drugs representing different mechanistic groups, indicating multiple mechanisms of action of the benzimidazoles.

Drug resistance

Drugs with defined mechanisms of resistance mostly showed RFs in the 10-fold to several hundred-fold range (Table 5). In comparison, benomyl showed an RF of only 2–3 for P-glycoprotein, glutathione and tubulin associated resistance, and carbendazim had a top RF of close to 2 for tubulin associated resistance.

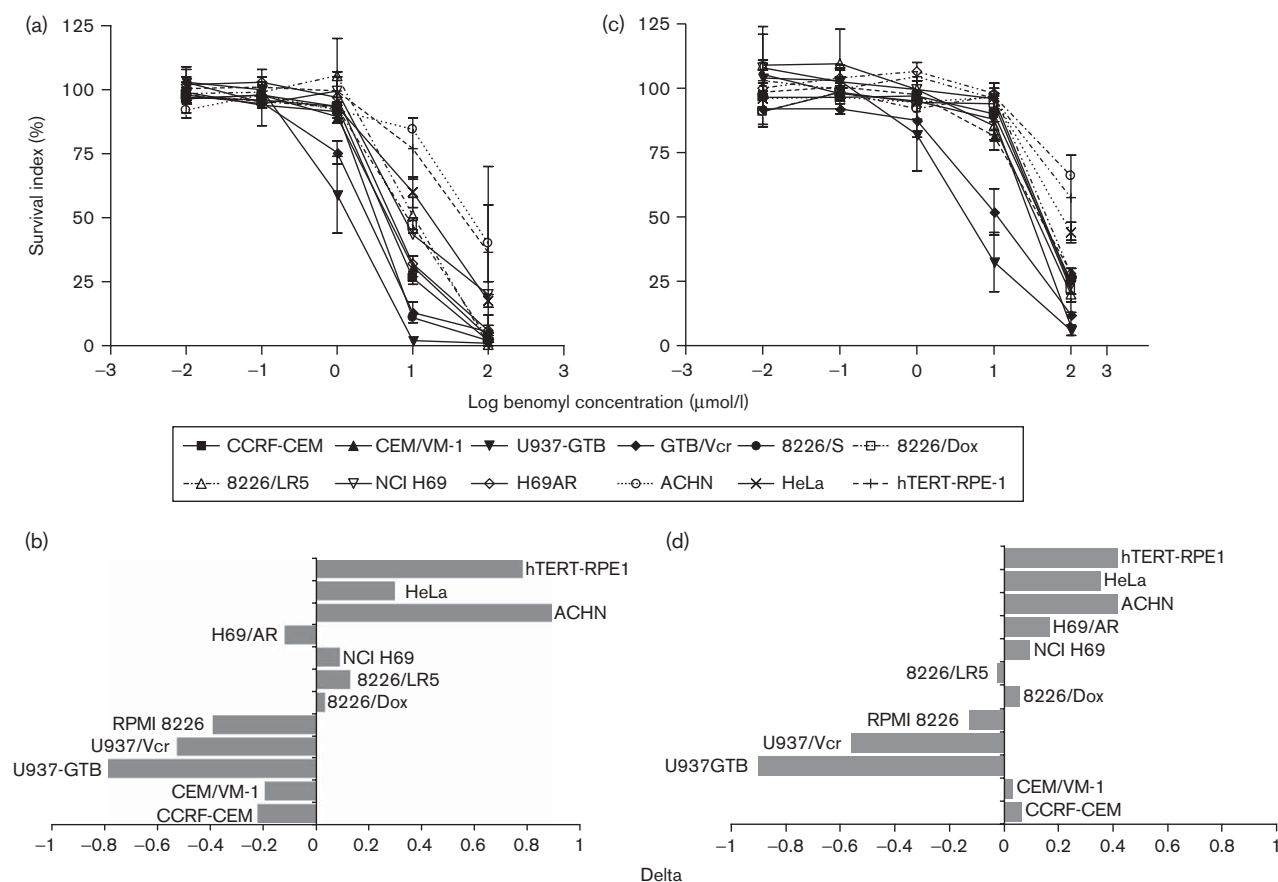
Gene expression approach to indicate mechanisms of action

A number of genes were found to be associated with the activity of benomyl and carbendazim based on cut-off correlation coefficients of ≥ 0.7 or ≤ -0.7 (Table 2). In general, there was good agreement for gene correlations between the two drugs, corroborating their close relationship in molecular structure and activity.

In another approach to retrieve mechanistic information on cytotoxic drugs, we calculated drug–gene correlations for some key genes reported to be associated with the activity of known mechanistic groups of standard and experimental anticancer drugs (Table 3). This approach seemed able to correctly identify typical drugs to their expected mechanistic groups. Thus, colchicine would be classified as a tubulin active drug, cisplatin as a DNA interactive drug and decitabine as an epigenetically active drug, whereas the activity of rotenone as expected seemed to be related to oxidative stress. However, deviations from this pattern (e.g. paclitaxel and the topoisomerase inhibitors) were noted. One explanation might be that the genes selected for some classifications might not be the mechanistically pivotal ones.

On the basis of our observation on correlation to Top2A and Top2B genes, the correlations to drugs expected to be topoisomerase inhibitors were higher; thus based on those genes, benomyl and carbendazim could be speculated to be topoisomerase inhibitors as well. Using this approach, benomyl and carbendazim would rather be considered to be DNA interactive, oxidative stress inducing rather than tubulin active as proposed earlier [9], but also to act more ‘multimechanistically’ than most other cytotoxic drugs.

Fig. 2



Concentration-activity relationships (a, c) and delta plots (b, d) for benomyl (a, b) and carbendazim (c, d), respectively, in the human tumour cell line panel. The delta plot illustrates tumour cell lines that are relatively sensitive (bars deviating to the left of zero mean) and relatively resistant (bars deviating to the right of zero mean). Delta for individual cell line was obtained by converting its IC_{50} to a logarithm and subtracting it from the mean of the IC_{50} logarithms of all the cell lines included. Results are presented as mean values \pm standard error of the mean of three independent experiments.

Table 4 Correlation coefficients between some cytotoxic drugs according to their main mechanism of action, and benomyl and carbendazim

Microtubule Inhibition	Benomyl	Carbendazim	Topoisomerase inhibition	Benomyl	Carbendazim
Benomyl	—	0.87	Beta-lapachone	0.80	0.57
Carbendazim	0.87	—	Etoposide	0.69	0.50
Vinblastine	0.71	0.62	Cryptolepine	0.68	0.50
Vincristine	0.64	0.54	Doxorubicin	0.64	0.66
Colchicine	0.61	0.56	Amsacrine	0.62	0.65
Paclitaxel	0.43	0.35	Mitoxantrone	0.60	0.87
Microtubule and respiratory chain inhibitors			Proteasome inhibitors		
Arsenic trioxide	0.88	0.65	Disulfiram	0.38	0.08
Podophyllotoxin	0.81	0.76	Bortezomib	0.55	0.77
Rotenone	0.75	0.62	Lactacystin	0.59	0.43
Fenbendazole	0.73	0.54			
Mebendazole	0.71	0.56			
Oxibendazole	0.68	0.59			
Antimetabolites			Alkylating agents		
6-Mercaptopurine	0.85	0.62	Carboplatin	0.75	0.71
5-Fluorouracil	0.64	0.53	Melphalan	0.72	0.58
Gemcitabine	0.37	0.47	Oxaliplatin	0.66	0.56
Fludarabine	0.49	0.73	Cisplatin	0.57	0.55
		Drugs with other mechanisms of action			
Anthracycline	0.83	0.81	Decitabine	0.65	0.93
Curcumin	0.73	0.57	Rapamycin	0.64	0.60

Table 5 Resistance factors for benomyl and carbendazim in comparison with those of some standard cytotoxic agents in the cell line panel used

Parental and resistant cell line pairs	CEM/VM1-/CCRF-CEM	U-937GTB/Vcr/U-937GTB	8226dox/RPMI 8226	8226LR5/RPMI 8226	H69AR/NCI-H69
Resistance mechanism	Topoisomerase-II-associated	Tubulin-associated	P-gp-associated	GSH-associated	MRP1-associated
Benomyl	1.07	1.83	2.65	3.31	0.62
Carbendazim	0.93	2.17	1.53	1.26	1.17
Vincristine	0.65	43.8	366	2.17	8.91
Doxorubicin	1.22	1.43	24.5	0.92	42.2
Etoposide	12.3	2.50	29.4	1.19	2.00
Melphalan	1.03	1.02	1.36	2.95	0.93

The resistance factor was calculated by dividing the IC₅₀ of the drug resistant subline with that of the parental cell line for each drug. GSH, reduced glutathione; MRP1, multidrug resistance-related protein 1 (also termed ABCC1); P-gp, P-glycoprotein.

Patient tumour cells

The patient tumour cells, essentially being nonproliferative *in vitro* were generally less sensitive to benomyl and carbendazim than the cell lines. IC₅₀ values were often not reached from the drug concentrations used (serial dilutions beginning with the highest concentration of 100 µmol/l). Thus, evaluation of activity in patient tumour cells was based on cell survival at the highest concentration used for benomyl and carbendazim, (Fig. 3).

As in the cell line panel, benomyl was more active than carbendazim in tumour samples from patients ($P < 0.0001$ in both solid and haematological malignancies). For benomyl, the mean \pm SEM SI for solid tumours was $42 \pm 4.8\%$, whereas the haematological malignancies tended to be more sensitive with a mean SI of $31 \pm 5.0\%$ ($P = 0.0643$). In contrast, carbendazim showed similar sensitivity in solid and haematological malignancies with a mean SI of 72 ± 4.0 and $70 \pm 4.6\%$ for solid tumours and haematological malignancies, respectively ($P = 0.8823$).

Discussion

Despite recent major progress in the basic science of cancer and the introduction in the clinic of 'targeted' anticancer drugs, progress in the medicinal treatment of cancer has been fairly slow, and no end to the utility of broad acting cytotoxic drugs is in sight [10]. In this context, drug molecules already in use for other therapeutic purposes could unveil potentially interesting properties and be suitable for the development of anti-cancer drugs.

Benomyl and carbendazim are not mutagenic and are relatively atoxic *in vivo* in laboratory mice [4]. The LD₅₀ values of benomyl and carbendazim in rodents are both high [11]. These observations in addition to proposed microtubule inhibitory activity of benomyl and carbendazim formed the background for the present investigation of benomyl and carbendazim, the latter already in phase 1 anticancer clinical trials with promising results [2,3].

We here expand earlier work on these molecules with respect to mechanisms of action and resistance, and also include mechanism-related gene expression correlation

profiles. Furthermore, this is the first report on the cytotoxic potential *in vitro* of benomyl and carbendazim using a model, that is, primary cultures of tumour cells from patients [5], which could more reliably indicate suitability as anticancer drugs as well as their pattern of diagnosis specific activity. The difference observed in activity profile in the patient samples is potentially clinically important, with carbendazim showing similar activity in solid tumours as in haematological malignancies. This is an unusual feature of anticancer drugs that should give priority to the clinical development of carbendazim rather than benomyl despite its lower potency. The somewhat lower drug resistance also argues in favour of carbendazim for further clinical development.

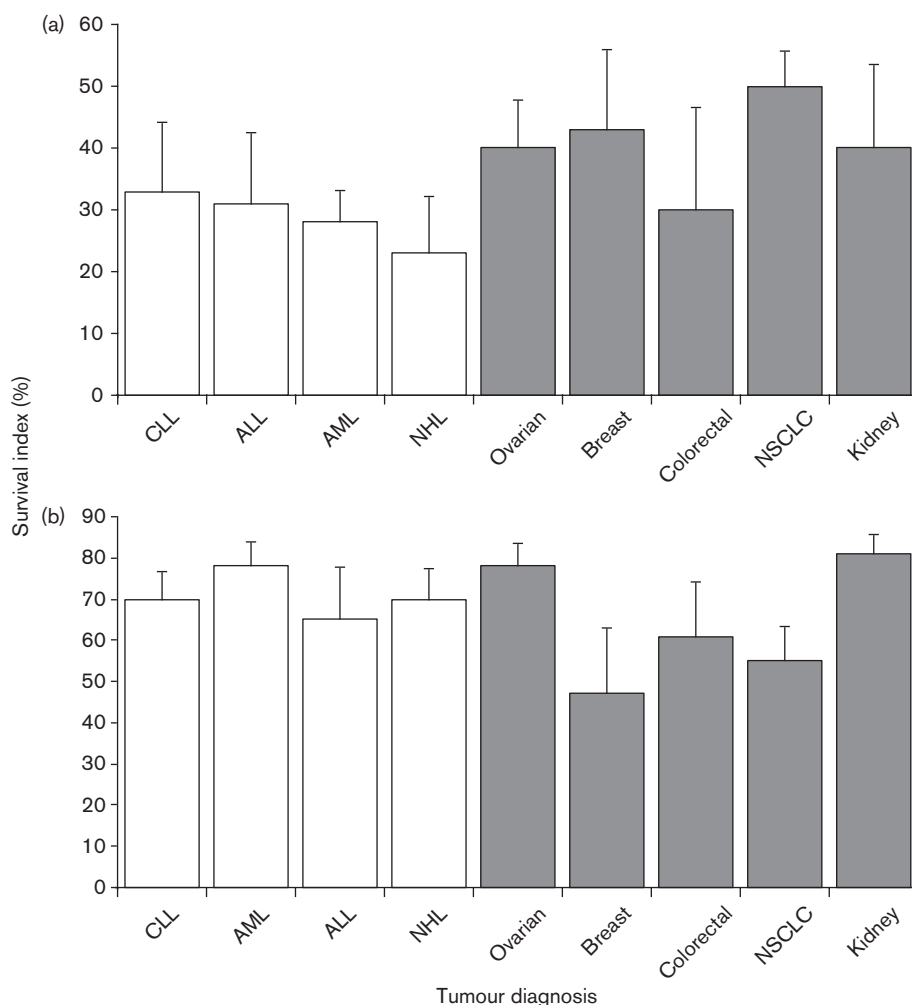
Benomyl and carbendazim showed similar activity spectrum and comparatively high correlations to various mechanisms of action, as indicated by the observations of generally high drug–drug activity and drug activity–gene expression correlations covering different mechanistic groups. These findings suggest that these benzimidazoles have diverse cytotoxic mechanisms of action.

The present results would suggest that these benzimidazoles, besides activity in the microtubule, might rather act preferentially on the DNA, inducing oxidative stress as dominant mechanisms of action rather than the putative tubulin activity they had been described for previously.

In support of this conclusion, we have performed *in-vivo* experiments earlier using various PET tracers and tritium-labelled thymidine after oral benomyl administration to mice (not shown). The results suggest that induction of chemical hypoxia occurred in various tissues, implying the generation of oxidative stress by benomyl, and thus possibly also by carbendazim.

It could be noted that the butylcarbamoyl side chain of benomyl yields mitochondria-active *n*-butyl isocyanate, which might explain the higher correlation of benomyl than carbendazim to rotenone. In contrast, the activity of the side chain might also explain the differential expression among drug activity–gene expression correlations between benomyl and carbendazim (e.g. for catalase, glutaredoxin and thioredoxin).

Fig. 3



Bar graph showing survival indices in patient tumour cells from the tumour types indicated for 100 $\mu\text{mol/l}$ benomyl (a) or carbendazim (b). The data presented are mean values \pm SEM for the number of samples included. ALL, acute lymphoblastic leukaemia; AML, acute myelocytic leukaemia; CLL, chronic lymphocytic leukaemia; NHL, non-Hodgkin's lymphoma; NSCLC, non-small-cell lung cancer.

The HIF-1- α gene, associated, in part, with chemical hypoxia and thus reactive oxygen species formation, showed equally high correlations to both benomyl and carbendazim. However, considering genes generally associated with reactive oxygen species-associated stress, we found somewhat higher drug activity–gene expression correlations for benomyl compared with carbendazim, which could be in agreement with previous *n*-butyl isocyanate-related observations [12].

Carbendazim has been regarded as microtubule inhibiting. However, our results indicate that carbendazim may rather target DNA and induce oxidative stress and epigenetic regulation. Interestingly, mitoxantrone has been reported to be a DNA hypomethylating agent besides its known antitopoisomerase activity [13], and carbendazim showed high mechanistic correlation to

mitoxantrone. Interestingly, benzimidazoles have been recently proposed to be histone deacetylase inhibitors [14]. Similar to carbendazim, benomyl might be topoisomerase inhibiting considering its high mechanistic correlation to β -lapachone and the doxorubicin-like drug activity gene expression profile for the topoisomerase gene isoforms α and β ; however, this activity might be less strong compared with its alkylating properties until biotransformed to carbendazim.

Overall, the present results indicating multiple mechanisms of action for benomyl and carbendazim support their further development and use as single drugs. In contrast, their optimal combinations with other anti-cancer drugs do not follow easily from the present findings and need to be empirically explored in clinically relevant preclinical models.

The current approach of elucidating the mechanism of action of a cytotoxic molecule, that is, looking for similarity of the activity of drugs with more or less well-defined mechanisms, and looking for correlative associations with a broad array of genes certainly, has strengths and limitations. The major strength lies in the provision of a broad array of possible mechanisms of action, and has been applied recently to pinpoint the drug resistance mechanism in the 8226 myeloma cell line [15]. However, the approach does not provide proofs of a mechanism of action but rather generates hypotheses that need to be addressed by direct tests *in vitro*.

Currently, we are testing another way to approach the question of drug mechanisms of action by comparing the change in gene expression pattern produced by the molecule to that of mechanistically better characterized drugs as recently described in the connectivity map approach [16]. In the first step of this approach, we intend producing a carbendazim-induced 'gene perturbation' pattern in the MCF-7 breast cancer cell line and will subsequently use the connectivity map to look for testable clues to its mechanism of action.

Our present findings together with those made earlier make it conceivable that benomyl and carbendazim might be suitable for the development of anticancer drugs. Overall, the properties of benomyl and carbendazim observed in this study, including a broad mechanistic spectrum, low RFs, interesting activity profiles in patient tumour cells together with earlier observations of good in-vivo tolerance as well as the novel discoveries made merits further development of benomyl and carbendazim as anticancer drugs.

Acknowledgements

The authors are grateful to Malin Wickström and Linda Rickardson for database support. Excellent bioinformatics support was provided by Hanna Göransson and expert technical assistance was provided by Lena Lenhammar and Christina Leek. This study was financially supported by the Swedish Cancer Society and the Lions Cancer Research Fund.

References

- 1 Monico-Pifarre A, Xirau-Vayreda M. Study of carbendazim residue accumulation on greenhouse and field-grown strawberries, after successive treatments with benomyl. *J Assoc Off Anal Chem* 1990; **73**:553–556.
- 2 Britten CD, Delioukina M, Boulos L, Reiswig L, Gicanov N, Rizzo J, *et al*. A phase I and pharmacokinetic (PK) study of FB642 administered orally on daily schedule to patients with advanced solid tumors. 2001 ASCO Annual Meeting 2001.
- 3 Hao D, Rowinsky E, Rizzo J, Rosen L, Felton S, Smetzer L, *et al*. A phase I and pharmacokinetic (PK) study of FB642 administered orally on a weekly schedule to patients (Pts) with advanced solid tumors. 2000 ASCO Annual Meeting 19: 2000 (Abstract 818).
- 4 Hellman B, Laryea D. Inhibitory action of benzimidazole fungicides on the in vivo incorporation of [3H]thymidine in various organs of the mouse. *Food Chem Toxicol* 1990; **28**:701–706.
- 5 Csoka K, Larsson R, Tholander B, Gerdin E, de la Torre M, Nygren P. Cytotoxic drug sensitivity testing of tumor cells from patients with ovarian carcinoma using the fluorometric microculture cytotoxicity assay (FMCA). *Gynecol Oncol* 1994; **54**:163–170.
- 6 Larsson R, Nygren P. Pharmacological modification of multi-drug resistance (MDR) in vitro detected by a novel fluorometric microculture cytotoxicity assay. Reversal of resistance and selective cytotoxic actions of cyclosporin A and verapamil on MDR leukemia T-cells. *Int J Cancer* 1990; **46**:67–72.
- 7 Rickardson L, Fryknas M, Dhar S, Lovborg H, Gullbo J, Rydaker M, *et al*. Identification of molecular mechanisms for cellular drug resistance by combining drug activity and gene expression profiles. *Br J Cancer* 2005; **93**:483–492.
- 8 Dhar S, Nygren P, Csoka K, Botling J, Nilsson K, Larsson R. Anti-cancer drug characterisation using a human cell line panel representing defined types of drug resistance. *Br J Cancer* 1996; **74**:888–896.
- 9 Winder BS, Strandgaard CS, Miller MG. The role of GTP binding and microtubule-associated proteins in the inhibition of microtubule assembly by carbendazim. *Toxicol Sci* 2001; **59**:138–146.
- 10 Nygren P, Larsson R. Overview of the clinical efficacy of investigational anticancer drugs. *J Intern Med* 2003; **253**:46–75.
- 11 Rehnberg GL, Cooper RL, Goldman JM, Gray LE, Hein JF, McElroy WK. Serum and testicular testosterone and androgen binding protein profiles following subchronic treatment with carbendazim. *Toxicol Appl Pharmacol* 1989; **101**:55–61.
- 12 Kroes RA, Abravaya K, Seidenfeld J, Morimoto RI. Selective activation of human heat shock gene transcription by nitrosourea antitumor drugs mediated by isocyanate-induced damage and activation of heat shock transcription factor. *Proc Natl Acad Sci U S A* 1991; **88**:4825–4829.
- 13 Parker BS, Cutts SM, Nudelman A, Rephaeli A, Phillips DR, Sukumar S. Mitoxantrone mediates demethylation and reexpression of cyclin d2, estrogen receptor and 14.3.3sigma in breast cancer cells. *Cancer Biol Ther* 2003; **2**:259–263.
- 14 Manku S, Allan M, Nguyen N, Ajamian A, Rodrigue J, Therrien E, *et al*. Synthesis and evaluation of lysine derived sulfamides as histone deacetylase inhibitors. *Bioorg Med Chem Lett* 2009; **19**:1866–1870.
- 15 Fryknas M, Dhar S, Oberg F, Rickardson L, Rydaker M, Göransson H, *et al*. STAT1 signaling is associated with acquired crossresistance to doxorubicin and radiation in myeloma cell lines. *Int J Cancer* 2007; **120**:189–195.
- 16 Lamb J, Crawford ED, Peck D, Modell JW, Blat IC, Wrobel MJ, *et al*. The Connectivity Map: using gene-expression signatures to connect small molecules, genes, and disease. *Science* 2006; **313**:1929–1935.